

Effects from Gold Electrodes on the Electron-Phonon Coupling of Poly(*p*-phenylenevinylene) Films

Eralci M. Therézio,^{*a} Ángel A. Hidalgo,^b Osvaldo N. Oliveira Jr.,^c Raigna A. Silva^d and Alexandre Marletta^d

^aDepartamento de Matemática, Universidade Federal de Mato Grosso, 78735-901 Rondonópolis-MT, Brazil

^bDepartamento de Física, Universidade Federal do Piauí, 64049-690 Teresina-PI, Brazil

^cInstituto de Física de São Carlos, Universidade de São Paulo, CP 369, 13560-970 São Carlos-SP, Brazil

^dInstituto de Física, Universidade Federal de Uberlândia, CP 593, 38400-902 Uberlândia-MG, Brazil

Interface effects between metal electrodes and organic films are crucial for the overall performance of organic electronics devices. We investigate effects from gold electrodes deposited on spin-coated films of poly(*p*-phenylene vinylene) (PPV). While a thin Au layer (16 nm) did not affect the absorption and emission spectra of PPV, a 64 nm thick Au layer induced blue shifts in both spectra owing to the reduction in the effective conjugation degree of PPV segments. Upon combining photoluminescence and Raman scattering spectroscopies, we noted that the Au clusters interact preferentially with the phenyl rings of the polymer chain, leading to shifts in the vibrational modes at 1100 and 555 cm⁻¹ and a significant change in the electron-phonon coupling inferred from the Huang-Rhys parameters. These results are consistent with theoretical predictions in *ab initio* calculations, which imply that the final properties of polymeric devices may be tuned with adequate conditions for electrode deposition.

Keywords: poly(*p*-phenylene vinylene), metal/polymer interface, electronic structure

Introduction

Conjugated polymers can be used in emissive layers in polymer light emitting diodes (PLEDs), solar cells, and sensors.¹ The possible applications of poly(*p*-phenylene vinylene) (PPV) and its derivatives in flat colored displays triggered a number of fundamental studies on the physical processes in emissive devices,¹⁻³ most of which comprise a polymer layer between two metal films. The latter may serve either as electrodes for charge injection in electroluminescent devices or mirrors in cavities to manipulate the radiative properties of the emissive species in the polymer. The electronic and optoelectronic properties of the emissive layer depend, basically, on film processing and polymer/metal interactions,²⁻⁶ with the active layer having a thickness of the order of the wavelength. Becker *et al.*⁷ addressed the problem of thickness-related interference in such devices, with emphasis on the angular intensity distribution. Moreover, the effect of the cavity, when photoluminescence measurements are carried out

with normal and back scattered geometry and the diffraction index of the substrate is ca. 1.5 (glass), is decreased substantially and the Beer-Lambert law is valid.⁸ The control of the interplay between radiative and non-radiative decay processes is crucial for developing highly efficient devices, which is still a difficult task as many processes are not understood in detail. For instance, the effect from the metal layers on the vibronic structure of the emission spectra is a matter of debate in the literature.

In this paper we studied the effect from varying the thickness of an Au layer deposited on spin-coated PPV films. The vibronic structure in the emission spectra was used to determine the electron-phonon coupling (Huang-Rhys factor, *S*) and the energy difference between the vibronic bands of the active phonons. Three effective phonons are believed to be responsible for the vibrational bands. The parameter *S* was estimated fitting the emission spectra for all sample conditions in the scope of the semi-empirical molecular-exciton theory. Raman spectroscopy was performed to investigate the vibrational modes (ca. 550 and ca. 1100 cm⁻¹) in the Au/PPV system. The investigation of the Au electrode serves as a fundamental study for

*e-mail: therezio@ufmt.br, therezio@gmail.com

applying reverse electrodes in solar cells because the organic interfacial layer at metal/inorganic semiconductor structures plays an important role in determining the main parameters of the devices.^{9,10}

Experimental

PPV films were obtained from the soluble precursor poly(xylylidene tetrahydrothiophenium chloride) (PTHT) that was thermally converted into PPV at high temperatures ($> 200\text{ }^{\circ}\text{C}$). Figure 1 shows the chemical structure of PTHT and PPV monomers and the thermal conversion process. Spin-coated films of PTHT on glass substrates (BK7) were obtained and thermally converted to PPV under vacuum (10^{-3} torr) at $230\text{ }^{\circ}\text{C}$ during 2 h. After thermal conversion, the Au film was deposited on top of the polymer film. To facilitate analyzing the spectral effects, only one-half of the PPV film was covered with the Au film evaporated at a pressure of 10^{-1} mbar, and therefore with the same sample we could analyze the spectra with and without the Au layer. The Au film had two values of thickness, viz., 16 nm (referred to as Au-thin) and 64 nm (Au-thick), whereas the PPV film had the same thickness in the two samples. Figure 2 shows the layout of the BK7/PPV/Au films.

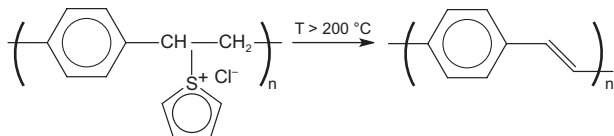


Figure 1. Thermal conversion procedure for PPV.

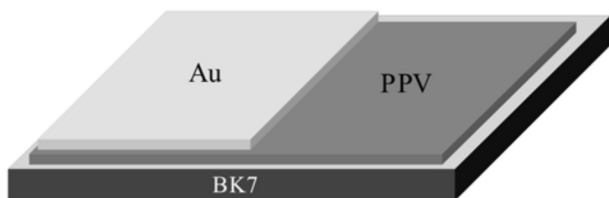


Figure 2. Layout of the BK7/PPV/Au-thin or Au-thick films.

The absorption spectra in the UV-Vis region were taken with a Shimadzu UV-2501PC spectrometer. For the photoluminescence (PL) spectra an Ocean-optics USB 2000 spectrometer was used, with the samples placed in a cryostat under 10^{-3} mbar. The 458 nm line of an argon ion laser was the excitation source. To avoid interference effects and wave guiding of the emitted light, the samples, the laser beam and the spectrometer were kept at a fixed geometry during the experiments.⁷ The Raman spectra were recorded from 200 to 1800 cm^{-1} with a multichannel Jobin-Yvon T 64000 spectrometer equipped with a cooled charge-coupled device (CCD) detector. The scattering signal was collected

in the backscattering configuration under a microscope using the excitation laser line at 514.5 nm with a spectral resolution of 4 cm^{-1} .

Results and Discussion

Figures 3a and 3b show the absorbance spectra in the UV-Vis range for BK7/PPV, BK7/PPV/Au-thin and BK7/PPV/Au-thick films. Basically, the absorbance line shape is associated with a non-local transition ($\pi \rightarrow \pi^*$) of PPV segments according to the molecular exciton model.¹¹ The thin Au layer does not affect the absorbance spectrum of PPV, with the statistical distribution of conjugation lengths being preserved. In contrast, the thick Au layer caused a blue shift - owing to a decrease in the effective PPV conjugation degree - and broadening of the absorbance spectrum in comparison with the PPV layer. A similar effect was observed for PPV and derivatives degraded by photo-oxidation,¹² which was attributed to the generation of carbonyl (C=O) groups. The latter defects induced a decrease in the conjugation degree along the polymer main chain, and therefore we may infer that in this study the interaction between the metal and the phenylene can change the degree of conjugation.

The PPV normalized photoluminescence spectra at 10 and 300 K are shown in Figure 4. For the Au-thin film, the line shape of PPV emission does not change significantly (Figure 4a), and the broadening of the PL spectra at room temperature is attributed to an increased thermal disorder. In contrast, the Au-thick film displays significant changes in the PL spectrum. Since the samples were processed simultaneously, all films may be assumed to have similar average PPV conjugation lengths before the metal deposition (see the spectra in Figure 3). Therefore, the changes induced by the thick metal coating on the relative intensities of the emission bands, mainly at 550 nm, can be attributed to the coupling of the electron vibrational modes. In addition, the electronic structure of PPV was also affected with the increase in temperature, even for the Au-thin film, which caused the blue shift of 5 nm in the PL spectrum. For the Au-thick sample at low temperature, the PL spectrum in Figure 4b is blue-shifted by 4 nm in comparison with the PPV without the metallic film. Two possibilities can be considered: (i) the deposition of the thick Au film introduces structural defects along the PPV chains reducing the effective conjugation degree; or (ii) there is interaction between PPV and the Au clusters. Upon increasing the sample temperature, the Au-thick layer enhanced the coupling of the electron-vibrational modes and the peak position was almost the same for the two PPV samples with Au-thin and Au-thick layers.

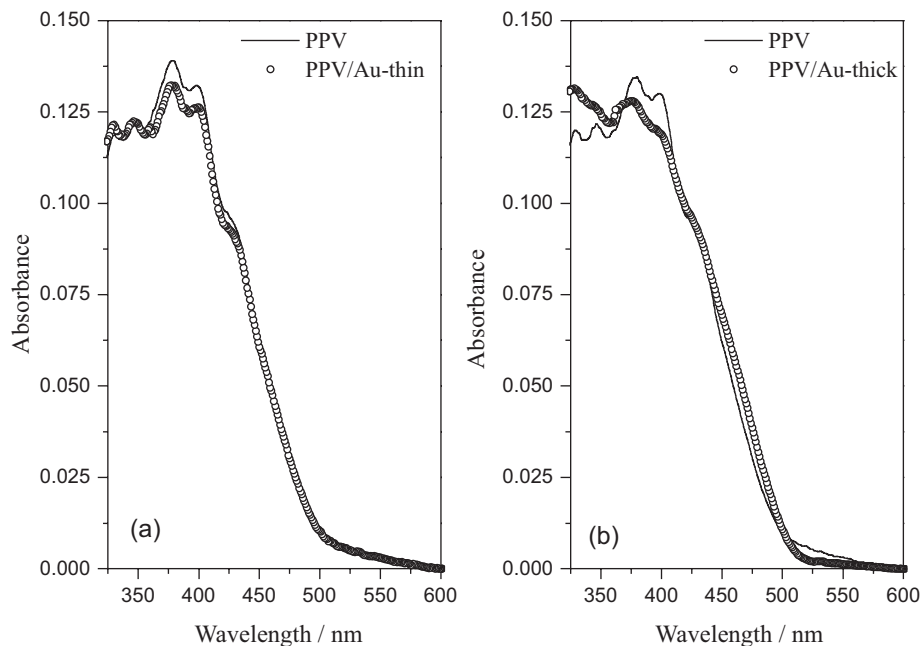


Figure 3. (a) Absorbance spectra for BK7/PPV and BK7/PPV/Au-thin film side. (b) Absorbance spectra for BK7/PPV and BK7/PPV/Au-thick film side. The solid line (—) represents the spectrum of the BK7/PPV side and the open circles (○) represent the spectra of the BK7/PPV/Au side.

Since emission of PPV takes place in segments with long conjugation degrees,¹³ the presence of the Au-thick layer reduced the effective PPV conjugation degree and increased the electron-phonon coupling.

The effects from the Au-layer on vibrational modes of PPV were investigated using Raman spectroscopy. The spectra in Figure 5a are similar to those of PPV derivatives,^{14,15} featuring two main bands at 550 and

1100 cm^{-1} . These vibrational modes appear in both infrared and Raman spectra, being assigned - according to theoretical calculations for PPV and derivatives - to C-H plus C-C ring out-of-plane bend (522 and 555 cm^{-1}) and C-H ring in-plane-bend (1005, 1135 and 1174 cm^{-1}).¹⁶ In principle, the C-C ring stretch at 1518, 1543, 1550 and 1584 cm^{-1} could have been observed in the Raman spectra, but this did not occur because their intensity is very small.

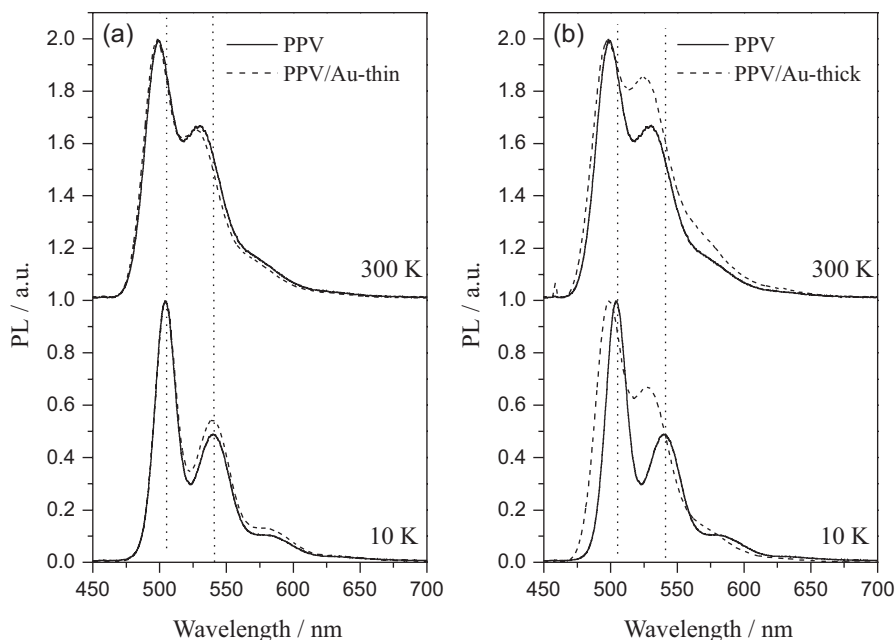


Figure 4. Normalized photoluminescence spectra at 10 and 300 K for (a) BK7/PPV/Au-thin and (b) BK7/PPV/Au-thick films. The PL spectra of BK7/PPV are given in both Figures for comparison. The solid lines (—) represent the spectra acquired on the BK7/PPV side and the dashed line (---) the spectra on the BK7/PPV/Au side.

In any case, the main changes caused by the Au layer occurred in the 800-1200 cm^{-1} range and at 550 cm^{-1} , as can be inferred from Figure 5. The experimental data were fitted using Lorentz curves considering the vibrational modes for PPV.¹⁴⁻¹⁷

According to theoretical calculations¹⁷ there is a red shift of ca. 10 cm^{-1} at the 1089 cm^{-1} band due to adsorption of Au on the phenyl ring, which is consistent with the experimental shift in the data of Figures 5b and 5c. There is also a distortion in the band at 555 cm^{-1} (see Figures 5d and 5e). The two bands at 549 and 574 cm^{-1} for pristine PPV are shifted in the PPV/Au-thick sample, being again consistent with theoretical calculations by Brito *et al.*¹⁷ that

pointed to adsorption of Au clusters on the phenyl ring. Calculations¹⁷ were made within the density functional theory (DFT), using the Perdew-Burke-Ernzerhof spin-polarized generalized gradient approximation scheme (PBE-GGA) to calculate the electron-electron interactions. For the structural, energetic, and electronic properties, the Au/PPV system was described with a supercell where the PPV chain comprised four PPV monomers in an orthorhombic supercell. The vibrational properties were obtained with the density functional perturbation theory (DFPT) approach, as implemented in the plane-wave self-consistent field (PWSCF) code, in order to include the polarizability effects on the vibrational modes and

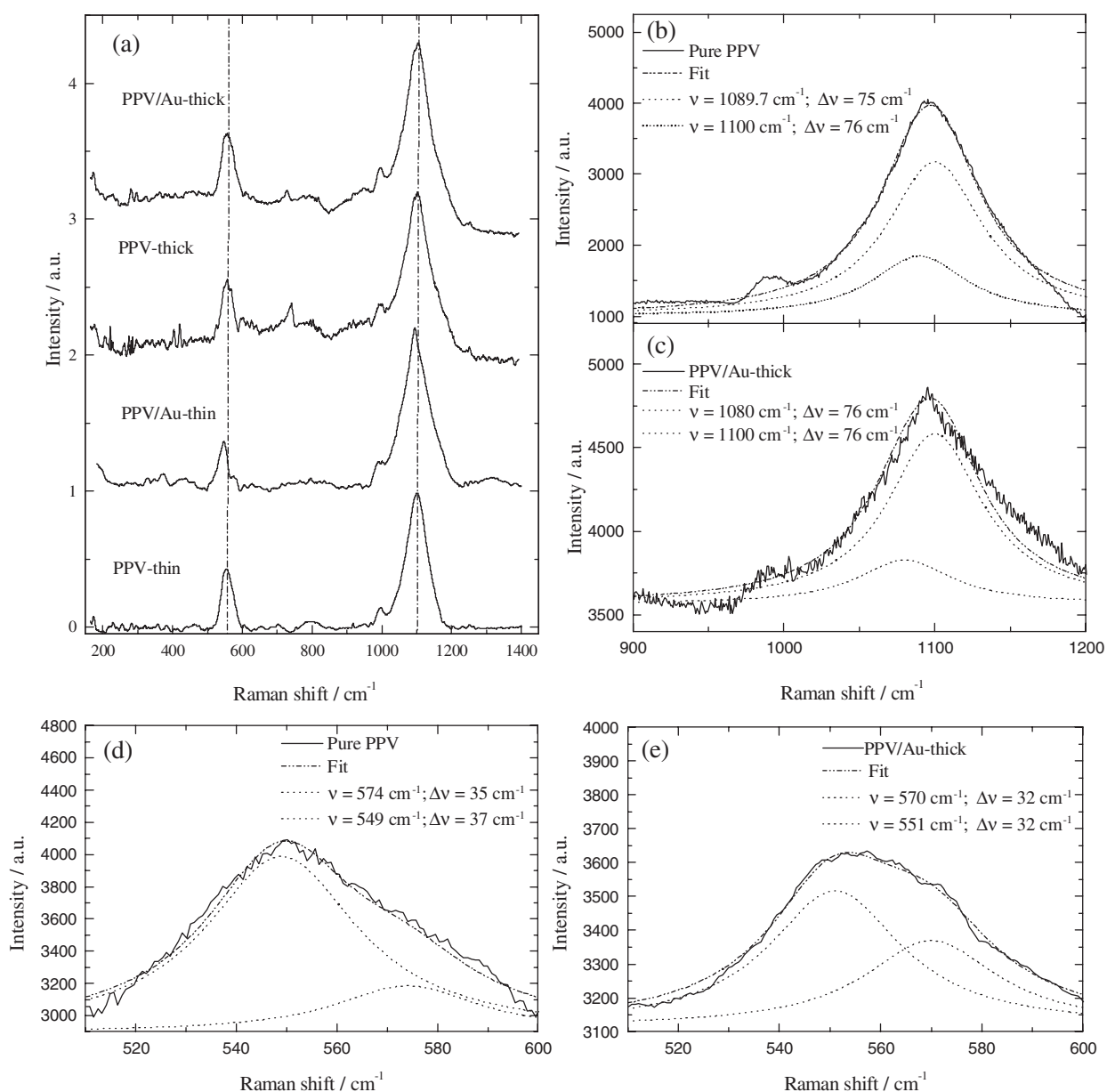


Figure 5. (a) Raman spectra for BK7/PPV, BK7/PPV/Au-thin, and BK7/PPV/Au-thick films in the range from 180 to 1400 cm^{-1} ; (b) Raman spectra of pristine PPV and (c) Au-PPV films in the range from 1000 to 1200 cm^{-1} ; (d) Raman spectra of pristine PPV and (e) Au-PPV films for the 555 cm^{-1} band.

Table 1. Fitting parameters: zero-phonon position (λ_{ab}), homogeneous line shape enlargement (d) and Huang-Rhys parameters S_1 , S_2 and S_3

Sample	Temperature / K	λ_{ab} / nm	d / cm^{-1}	S_1 $\nu_1 = 1500 \text{ cm}^{-1}$	S_2 $\nu_2 = 1100 \text{ cm}^{-1}$	S_3 $\nu_3 = 550 \text{ cm}^{-1}$
PPV	10	503	290	0.32	0.31	0.15
PPV	300	498	290	0.23	0.41	0.29
PPV/Au-thin	10	503	290	0.30	0.36	0.15
PPV/Au-thin	300	497	310	0.25	0.42	0.28
PPV/Au-thick	10	498	310	0.24	0.41	0.33
PPV/Au-thick	300	496	310	0.20	0.47	0.45

frequencies. For the PPV/Au-thin sample, the shift was not observed because the interaction between PPV and Au clusters should be weak. There was no significant difference between the Raman frequencies of pure PPV and Au-PPV films but the Raman bands in the range 1000-1200 cm^{-1} were slightly down-shifted by ca. 10 cm^{-1} owing to the interaction with phenyl rings, as mentioned above.

To estimate the electron-phonon coupling, the Huang-Rhys parameter was calculated from the PL spectra in Figure 4 within the Frank-Condon approximation, molecular exciton scope and pure displacement approximation, using equation 1:¹⁸⁻²¹

$$I_{ab}(\omega) = \frac{2a_m\pi\omega^3}{3c\hbar} |\bar{\mu}_{ab}|^2 \int_{-\infty}^{+\infty} dt \exp\left(it(\omega_{ab} - \omega) - \frac{d^2 t^2}{2}\right) \prod_j G_j(t) \quad (1)$$

where

$$G_j(t) = \exp\left[-\sum_{j=1}^N S_j \left\{ (\bar{n}_j + 1) \exp(it\omega_j) + \bar{n}_j (\exp(-it\omega_j) - 1) \right\}\right], \quad (2)$$

$\bar{\mu}_{ab}$ is the electric dipole matrix element, a_m describes the medium effect, c is the speed of light, $\hbar\omega_{ab} = E_b - E_a$ is the energy difference between the localized electronic states LUMO (E_b) and HOMO (E_a) of the copolymer segments with the largest conjugation degree, and d is the inhomogeneous spectral line for a Gaussian distribution. S_j is the electron-phonon coupling (Huang-Rhys parameter) for the j^{th} -phonon with energy ω_j and $\bar{n}_j = (\exp(\hbar\omega_j/2kT) - 1)^{-1}$ is the thermal occupation probability.

Figure 6 shows the simulated PL line shape obtained with equation 1 for the PL data of Figure 4. The adjustable parameters were the Huang-Rhys factor for three effective vibrational modes $\nu_1 = 1500 \text{ cm}^{-1}$, $\nu_2 = 1100 \text{ cm}^{-1}$, and $\nu_3 = 550 \text{ cm}^{-1}$. The parameters ω_{ab} (or λ_{ab}) and d were obtained directly from the electronic transition at ca. 500 nm. The three effective vibrational modes coupled with the electronic transitions were used as parameters, being respectively, S_1 , S_2 and S_3 . Table 1 displays the parameters used for the fitting. The Huang-Rhys parameter S_3 , associated with the C-H plus C-C ring out-of-plane bend,

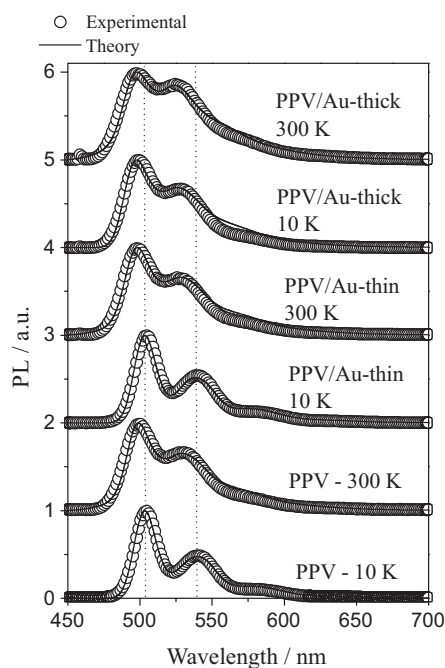


Figure 6. PPV emission spectra of BK7/PPV, BK7/PPV/Au-thin, and BK7/PPV/Au-thick films at room temperature (300 K) and 10 K. The open circles (\circ) represent the experimental data while the solid lines (—) represent theoretical fitting using equation 1 and the parameters in Table 1.

is the most affected, consistent with the experimentally observed distortion in the 555 cm^{-1} band of the Raman spectra (see Figures 5d and 5e). Similarly, the Huang-Rhys parameter S_2 changed significantly for the PPV/Au-thick sample, again corroborating the analysis of the Raman spectra and the *ab initio* calculations for gold adatoms and clusters interacting with PPV.¹⁷ Therefore the Au-layer affects mainly the modes related to the phenyl rings of PPV.

Conclusions

We have shown that the deposition of gold electrodes on PPV films may affect the polymer properties depending on the electrode thickness. In particular, a thick (64 nm) Au layer affected the PPV electronic structure by modifying the electron-phonon coupling, which then caused the

vibrational bands in the photoluminescence spectra to change. Through an analysis of Raman scattering data, it was inferred that Au clusters interacted preferentially with the phenylene rings of PPV. This conclusion was supported by a quantitative simulation of the emission line shape within the Franck-Condon approximation, in the scope of the molecular exciton theory.¹⁷ The Huang-Rhys parameter changed significantly for the vibrational mode with energy at 550 cm⁻¹ for the thick Au-layer, in agreement with the results from the Raman scattering spectroscopy.

The effects from the thickness of the gold electrode are also worth emphasizing, for it is possible to leave the PPV properties unaffected by depositing just a thin gold layer. It is likely that the optoelectronic properties can be controlled to some extent by varying either the electrode or the film thickness, which would represent an important step toward tailoring device characteristics. The most significant implication of these results is that one may predict effects from metallic electrodes deposited on polymer films, as the changes observed experimentally were consistent with the *ab initio* calculations where gold adatoms and clusters were made to interact with PPV.

Acknowledgements

The financial support from FAPESP, FAPEMIG, CAPES, CNPq and INEO (Brazil) is acknowledged.

References

1. Heeger, A. J. In *Conjugated Polymers and Related Materials. The Interconnection of Chemical and Electronic Structure*; Salanek, W. R.; Lundström, I.; Rånby, B., eds.; Oxford University Press: Oxford, 1993, pp. 27.
2. Greiner, A.; *Polym. Adv. Technol.* **1998**, *9*, 371.
3. Heeger, A. J.; Braun, D.; *US pat. 5869350* **1999** (CA 2105069A1).
4. Gebhardt, V.; Bacher, A.; Thelakkat, M.; Stalmach, U.; Meier, H.; Schmidt, H.-W.; Haarer, D.; *Adv. Mater.* **1999**, *11*, 119.
5. Wolf, H. C. In *Organic Molecular Aggregates*; Reineker, P.; Haken, H.; Wolf, H. C., eds.; Springer-Verlag: Berlin, 1983, pp. 49.
6. Wu, H.; Huang, F.; Peng, J.; Cao, Y.; *Org. Electron.* **2005**, *6*, 118.
7. Becker, H.; Burns, S. E.; Friend, R. H.; *Phys. Rev. B: Condens. Matter Mater. Phys.* **1997**, *56*, 1893.
8. Therézio, E. M.; Piovesan, E.; Anni, M.; Silva, R. A.; Oliveira, O. N.; Marletta, A.; *J. Appl. Phys.* **2011**, *110*, 44504.
9. Neugebauer, H.; Brabec, C.; Hummelen, J. C.; Sariciftci, N. S.; *Sol. Energy Mater. Sol. Cells* **2000**, *61*, 35.
10. Dökme, I.; Tunç, T.; Uslu, İ.; Altındal, Ş.; *Synth. Met.* **2011**, *161*, 474.
11. Marletta, A.; Gonçalves, V. C.; Balogh, D. T.; *J. Lumin.* **2006**, *116*, 87.
12. Gobato, Y. G.; Marletta, A.; Faria, R. M.; Guimaraes, F. E. G.; de Souza, J. M.; Pereira, E. C.; *Appl. Phys. Lett.* **2002**, *81*, 942.
13. Therézio, E. M.; Piovesan, E.; Vega, M. L.; Silva, R. A.; Oliveira, O. N.; Marletta, A.; *J. Polym. Sci., Part B: Polym. Phys.* **2011**, *49*, 206.
14. da Silva, M. A. T.; Dias, I. F. L.; Duarte, J. L.; Laureto, E.; Silvestre, I.; Cury, L. A.; Guimaraes, P. S. S.; *J. Chem. Phys.* **2008**, *128*, 94902.
15. Wantz, G.; Hirsch, L.; Huby, N.; Vignau, L.; Barriere, A. S.; Parneix, J. P.; *J. Appl. Phys.* **2005**, *97*, 34505.
16. Rakovic, D.; Kosticacuta, R.; Gribov, L. A.; Davidova, I. E.; *Phys. Rev. B: Condens. Matter Mater. Phys* **1990**, *41*, 10744.
17. Brito, W. H.; Silva, R. A.; Miwa, R. H.; *J. Chem. Phys.* **2010**, *133*, 204703.
18. Brailsford, A. D.; Chang, T. Y.; *J. Chem. Phys.* **1970**, *53*, 3108.
19. Chang, R.; Hsu, J. H.; Fann, W. S.; Liang, K. K.; Chang, C. H.; Hayashi, M.; Yu, J.; Lin, S. H.; Chang, E. C.; Chuang, K. R.; Chen, S. A.; *Chem. Phys. Lett.* **2000**, *317*, 142.
20. Marletta, A.; Guimaraes, F. E. G.; Faria, R. M.; *Braz. J. Phys.* **2002**, *32*, 570.
21. Yu, J.; Fann, W. S.; Kao, F. J.; Yang, D. Y.; Lin, S. H.; *Synth. Met.* **1994**, *66*, 143.

Submitted: May 1, 2015

Published online: June 23, 2015

FAPESP has sponsored the publication of this article.